

η -nuclear bound states revisited

E. Friedman^a, A. Gal^{a,*}, J. Mareš^b

^a*Racah Institute of Physics, The Hebrew University, 91904 Jerusalem, Israel*

^b*Nuclear Physics Institute, 25068 Řež, Czech Republic*

Abstract

The strong energy dependence of the s -wave ηN scattering amplitude at and below threshold, as evident in coupled-channels K -matrix fits and chiral models that incorporate the S_{11} $N^*(1535)$ resonance, is included self-consistently in η -nuclear bound-state calculations. This approach, applied recently in calculations of kaonic atoms and \bar{K} -nuclear bound states, is found to impose stronger constraints than ever on the onset of η -nuclear binding, with a minimum value of $\text{Re } a_{\eta N} \approx 0.9$ fm required to accommodate an η - ^4He bound state. Binding energies and widths of η -nuclear states are calculated within several underlying ηN models for nuclei across the periodic table, including $^{25}_{\eta}\text{Mg}$ for which some evidence was proposed in a recent COSY experiment.

Keywords:

meson-baryon interactions, mesons in nuclear matter, mesic nuclei

PACS: 13.75.Gx, 21.65.Jk, 21.85.+d

1. Introduction

Searches for meson-nuclear bound states have focused on K^- and η mesons, motivated by a general theoretical consensus that the near-threshold $\bar{K}N$ and ηN attraction generated by the s -wave resonances $\Lambda(1405)$ and $N^*(1535)$, respectively, translates into sufficiently attractive K^- -nucleus and η -nucleus interactions. A corollary of this resonance dominance is a strong energy dependence of the underlying $\bar{K}N$ and ηN interactions. Here we apply the lessons gained by handling the strong energy dependence of the near-threshold $\bar{K}N$ interaction in K^- -nuclear calculations [1] to η -nuclear

*Corresponding author: Avraham Gal, avragal@vms.huji.ac.il

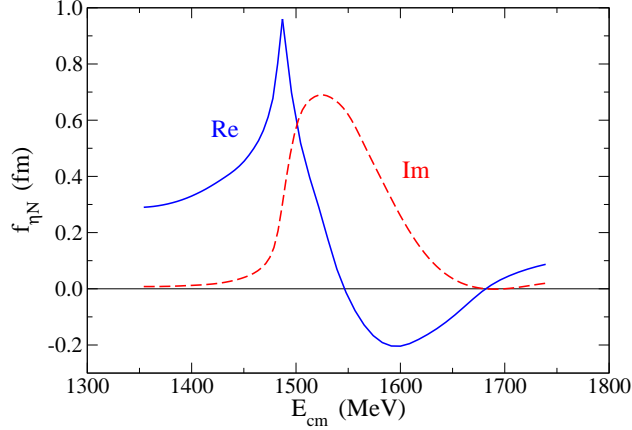


Figure 1: Energy dependence of the s -wave ηN cm scattering amplitude $f_{\eta N}(\sqrt{s})$, with scattering length $a_{\eta N} \equiv f_{\eta N}(\sqrt{s_{\text{th}}}) = 0.91(6) + i0.27(2)$ fm, as calculated by Green and Wycech (GW) fitting pion reaction and photoproduction data over a wide range of cm energies $E_{\text{cm}} (= \sqrt{s})$. The spike of $\text{Re } f$ is located at the ηN threshold, whereas $\text{Im } f$ peaks close to the $N^*(1535)$ mass. Figure adapted from Ref. [8].

bound-state calculations. Early calculations by Haider and Liu [2, 3] predicted η -nuclear bound states beginning with nuclear mass number $A \sim 12$. In these, as well as in a follow-up calculation [4], a fairly weak ηN attraction input was used, with $\text{Re } a_{\eta N} \lesssim 0.3$ fm, where $a_{\eta N}$ is the ηN scattering length. Several versions of coupled-channels chiral models [5, 6, 7] give similar values as well, whereas other models, particularly those using K -matrix methods to fit πN and γN reaction data in the $N^*(1535)$ resonance region, e.g. [8, 9, 10], yield considerably stronger ηN attraction with values of $\text{Re } a_{\eta N} \approx 1$ fm.¹ This might suggest that the onset of η -nuclear binding occurs already in the He isotopes for which strong final-state interaction precursors have been noted in proton- and deuteron-initiated η production [11, 12]. A robust pattern of η -nuclear bound states could yield useful information on the size of SU(3) flavor $\eta - \eta'$ mixing and about axial U(1) dynamics [13]. To date, however, experimental searches for such bound states have been unsuccessful, e.g. the latest negative results for ${}^3\text{He}$ (in photoproduction on ${}^3\text{He}$ [14]) and for ${}^4\text{He}$ (in $dd \rightarrow {}^3\text{He } p\pi^-$ [15]).

¹As for $\text{Im } a_{\eta N}$, it is constrained by $\pi N \rightarrow \eta N$ cross-section measurements, with values of $\text{Im } a_{\eta N} \sim 0.2\text{--}0.3$ fm in most theoretical analyses.

Regardless of the strong model dependence of $\text{Re } a_{\eta N}$, all studies of the ηN system near threshold, $\sqrt{s_{\text{th}}} = m_N + m_\eta \approx 1487$ MeV, agree that both real and imaginary parts of the s -wave center-of-mass (cm) scattering amplitude $f_{\eta N}$ decrease steeply in going subthreshold, as illustrated in Fig. 1. Since the in-medium ηN interaction relevant to the evaluation of η -nuclear bound states involves subthreshold ηN configurations, a procedure for going subthreshold is mandatory. Previous calculations focused on shifting the energy variable of $f_{\eta N}(\sqrt{s})$ or its in-medium version by a fixed amount below threshold: $\delta\sqrt{s} = -30$ MeV was found in Ref. [4] to provide a good approximation to a variety of off-shell effects, whereas $\delta\sqrt{s} = -B_\eta$, with B_η the η -nuclear binding energy, was used in Refs. [16, 17]. The latter procedure requires a self-consistent calculation to ensure that the B_η argument of the input $f_{\eta N}$ coincides with the B_η output of the binding energy calculation. However, it was shown in our recent studies of K^- -nuclear dynamics [18, 19, 20, 21, 22, 23] that a more involved self-consistent calculation is required to correctly implement the subthreshold energy dependence, and it is this self-consistent procedure that is applied here to calculate η -nuclear bound states. This procedure results in imposing stronger constraints than ever on the onset of η -nuclear binding.

Table 1: ηN scattering length $a_{\eta N}$ (in fm) in three coupled-channels models used in the present work. M1 and M2 correspond to versions I and II, respectively, of ηN amplitudes from the recent chiral-model work by Mai et al. [7], and GW denotes the K -matrix ηN amplitude due to Green and Wycech [8] shown in Fig. 1.

Model	$\text{Re } a_{\eta N}$	$\text{Im } a_{\eta N}$
M1	0.22	0.24
M2	0.38	0.20
GW	0.96	0.26

Below we proceed to describe briefly the self-consistent procedure used to handle the subthreshold energy dependence of the ηN amplitude for bound nucleons, and its embedding into a dynamical Relativistic Mean Field (RMF) scheme which allows for the first time to consider the polarization of the core nucleus by the bound η meson. To span a broad range of bound-state scenarios we apply our methodology to three distinct ηN amplitude models, with threshold values listed in Table 1. These amplitudes differ primarily

in the value of the real part, while their shape below threshold exhibits a substantial decrease particularly for $\text{Im } a_{\eta N}$, as illustrated for the GW amplitude model [8] in Fig. 1. We have calculated η -nuclear bound states across the periodic table for these three amplitude models, as reported and discussed here for $1s_\eta$ states. Finally, we also confront our results with a recent experimental suggestion of a $^{25}_\eta\text{Mg}$ bound state [24].

2. Methodology

In close analogy to the latest calculation of K^- -nuclear bound states [21], we calculate η -nuclear bound states by solving self-consistently the Klein-Gordon (KG) equation

$$[\nabla^2 + \tilde{\omega}_\eta^2 - m_\eta^2 - \Pi_\eta(\omega_\eta, \rho)] \psi = 0, \quad (1)$$

where $\tilde{\omega}_\eta = \omega_\eta - i\Gamma_\eta/2$ and $\omega_\eta = m_\eta - B_\eta$, with B_η and Γ_η the binding energy and the width of the η -nuclear bound state. The self-energy operator Π_η is related to a density- and energy-dependent optical potential V_η which is given by the following “ $t\rho$ ” form:

$$\Pi_\eta(\omega_\eta, \rho) \equiv 2\omega_\eta V_\eta = -4\pi F_{\eta N}(\sqrt{s}, \rho)\rho, \quad (2)$$

where $s = (E_\eta + E_N)^2 - (\vec{p}_\eta + \vec{p}_N)^2$ is the Lorentz invariant Mandelstam variable s which reduces to the square of the total ηN energy in the two-body cm frame and $F_{\eta N}$ is the in-medium ηN s -wave scattering amplitude in the lab system. Note that for $A \gg 1$ the lab system approximates well the η -nucleus cm system. Our in-medium $F_{\eta N}$ accounts for Pauli correlations in the Ericson-Ericson multiple-scattering approach, as reformulated in Ref. [25] and used recently in Ref. [23]:

$$F_{\eta N}(\sqrt{s}, \rho) = \frac{\tilde{f}_{\eta N}(\sqrt{s})}{1 + \xi(\rho)\tilde{f}_{\eta N}(\sqrt{s})\rho}, \quad \xi(\rho) = \frac{9\pi}{4p_F^2}, \quad (3)$$

where $\tilde{f}_{\eta N}(\sqrt{s}) = (\sqrt{s}/m_N)f_{\eta N}(\sqrt{s})$, with the kinematical factor \sqrt{s}/m_N transforming f from the two-body cm frame to the lab \tilde{f} , and where p_F is the local Fermi momentum corresponding to density $\rho = 2p_F^3/(3\pi^2)$. Note that $F_{\eta N}(\sqrt{s}, \rho) \rightarrow \tilde{f}_{\eta N}(\sqrt{s})$ upon $\rho \rightarrow 0$, as required by the low-density limit. Extensions of Eq. (3) to coupled channels and inclusion of self-energies do not change the results presented here in any qualitative way and will be discussed elsewhere [26].

In specifying the two-body cm energy \sqrt{s} appearing in Eq. (3) we recall that $s = (\sqrt{s_{\text{th}}} - B_\eta - B_N)^2 - (\vec{p}_\eta + \vec{p}_N)^2$, where the momentum-dependent term provides additional downward energy shift to that arising from the sum of binding energies $B_\eta + B_N$. Unlike in the free-space ηN cm system where $(\vec{p}_\eta + \vec{p}_N)_{\text{cm}} = 0$, this term in the lab system was found to contribute substantially in realistic nuclear applications [18, 19]. It has been verified numerically by us that $(\vec{p}_\eta + \vec{p}_N)^2$ is well approximated by its angle-average $(p_\eta^2 + p_N^2)$. Near threshold, then, to leading order in binding energies and kinetic energies with respect to masses, one obtains

$$\sqrt{s} \approx \sqrt{s_{\text{th}}} - B_N - B_\eta - \xi_N \frac{p_N^2}{2m_N} - \xi_\eta \frac{p_\eta^2}{2m_\eta}, \quad (4)$$

where $\xi_{N(\eta)} \equiv m_{N(\eta)}/(m_N + m_\eta)$. To transform momentum dependence into density dependence, the nucleon kinetic energy $p_N^2/(2m_N)$ is approximated within the Fermi gas model by $T_N(\rho/\rho_0)^{2/3}$, with average bound-nucleon kinetic energy $T_N = 23.0$ MeV, and the η kinetic energy $p_\eta^2/(2m_\eta)$ is substituted within the local density approximation by $-B_\eta - \text{Re } V_\eta(\sqrt{s}, \rho)$. Thus, the *in-medium* $\sqrt{s} = \sqrt{s_{\text{th}}} + \delta\sqrt{s}$ energy argument of $F_{\eta N}$ in Eq. (3) is density-dependent, with a form adjusted to respect the low-density limit, $\delta\sqrt{s} \rightarrow 0$ with $\rho \rightarrow 0$, as used recently in K^- -atom studies [23]:

$$\delta\sqrt{s} \approx -B_N \frac{\rho}{\bar{\rho}} - \xi_N B_\eta \frac{\rho}{\rho_0} - \xi_N T_N \left(\frac{\rho}{\rho_0}\right)^{2/3} + \xi_\eta \text{Re } V_\eta(\sqrt{s}, \rho). \quad (5)$$

Here $B_N \approx 8.5$ MeV is an average nucleon binding energy and ρ_0 ($\bar{\rho}$) is the maximal (average) nuclear density. The appearance of the V_η term due to $p_\eta \neq 0$ in finite nuclei contrasts with the common assumption $p_\eta = 0$ made in nuclear matter calculations. The dependence of V_η on energy through \sqrt{s} and on density ρ is explicitly marked in this expression. Note that for an attractive V_η and as long as $\rho \neq 0$, the shift of the two-body energy away from threshold is negative definite, $\delta\sqrt{s} < 0$, even as $B_\eta \rightarrow 0$. For a given B_η , neither \sqrt{s} nor V_η can be evaluated separately, implying that V_η is to be constructed *self-consistently* together with \sqrt{s} , which takes typically about 5 cycles of iteration. Once $V_\eta(\sqrt{s}, \rho)$ has been determined, it is used in the KG Eq. (1) to solve for the binding energy *eigenvalue* $B_\eta^{(n\ell)}$ in the η -nuclear $n\ell$ single-particle state. While varying the value of $B_\eta^{(n\ell)}$ in this process, the self-consistent requirement Eq. (5) is imposed at each step of the calculation of the eigenvalue.

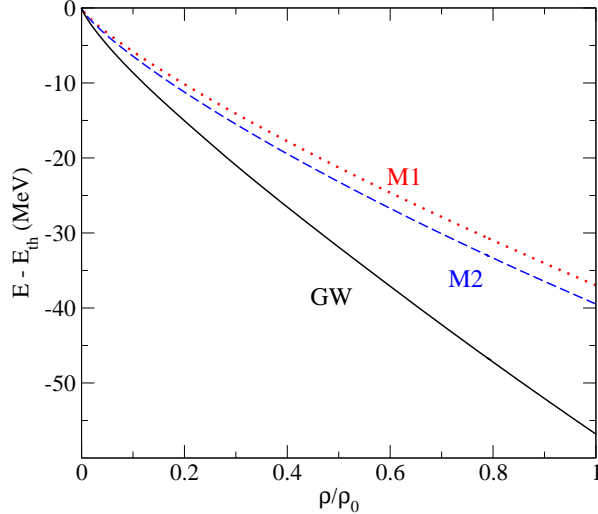


Figure 2: Subthreshold ηN energies probed by the η -nuclear potential as a function of the relative nuclear RMF density in Ca. Each of the three curves was calculated self-consistently according to Eq. (5) for a specific version of ηN subthreshold amplitude model, see text.

In Fig. 2 we show the downward subthreshold energy shift $\delta\sqrt{s} \equiv E - E_{\text{th}}$ as a function of the nuclear RMF density ρ in Ca, calculated self-consistently according to Eq. (5) for ηN amplitude models M1, M2 and GW (see Table 1). The hierarchy of the three curves reflects the strength of the input $\text{Re } f_{\eta N}(\sqrt{s})$ in the subthreshold region, with threshold values listed in Table 1. It is clear that downward energy shifts of up to ≈ 55 MeV are involved in the present self-consistent calculations.

3. Results and discussion

The methodology described in the last section was used to solve the KG equation (1) for η -nuclear bound states across the periodic table. In this Letter we highlight the systematics of the $1s_\eta$ bound state and compare our treatment of subthreshold energy dependence with previous studies. A more detailed account plus extensions are given elsewhere [26]. Three representative ηN amplitude models M1, M2 and GW (see Table 1) are employed here in order to span a wide range of ηN interaction strengths. Our main results are shown in Fig. 3 for binding energies B_η and widths Γ_η calculated

for $1s_\eta$ nuclear states in core nuclei from ^{12}C to ^{208}Pb . RMF equations of motion, along with the KG equation (1), are solved self-consistently [27], thereby allowing for core polarization by the η meson (see Ref. [19] for the latest application to K^- mesons). The core polarization effect on B_η and Γ_η was found in all cases displayed here to be less than 1 MeV. Therefore, the use of static nuclear densities is acceptable for not-too-light nuclear cores.

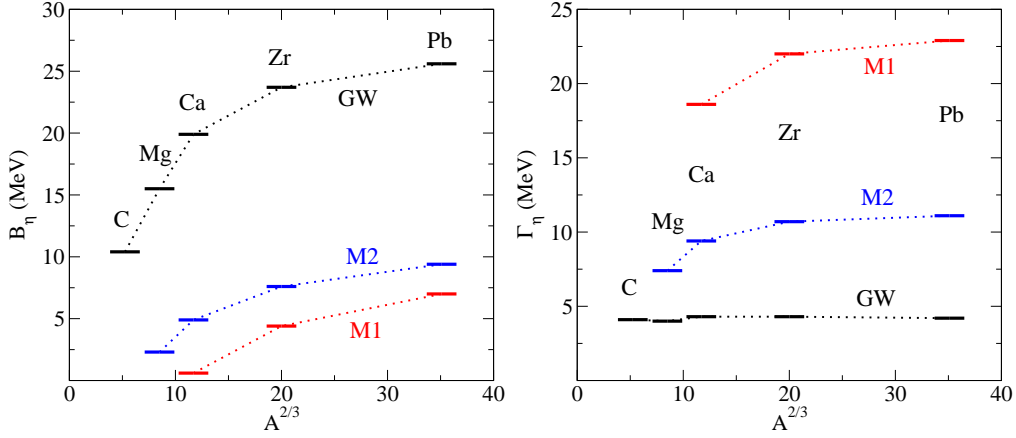


Figure 3: Binding energies (left) and widths (right) of $1s_\eta$ nuclear states across the periodic table calculated self-consistently using the M1, M2 and GW subthreshold ηN scattering amplitudes within a dynamical RMF scheme, see text.

Inspection of the l.h.s. of Fig. 3 reveals that for each of the three input ηN amplitude models the binding energy increases with A and appears to saturate for large values of A . As in Fig. 2, here too the hierarchy of the three curves reflects the strength of the $\text{Re } f_{\eta N}(\sqrt{s})$ input in the subthreshold region, with threshold values listed in Table 1. The M1 and M2 amplitudes are too weak to produce a $1s_\eta$ bound state in ^{12}C , with the onset of binding for the weaker M1 amplitude deferred to around ^{40}Ca . Of our three representative amplitudes, M1 is the closest one on shell to the Haider-Liu standard amplitude [2, 3, 4] which was used by these authors to argue for ^{12}C as the approximate onset of η -nuclear binding. In contrast, $\text{Re } f_{\eta N}(\sqrt{s})$ of the GW model is sufficiently strong to bind the $1s_\eta$ state in ^{12}C and in lighter core nuclei, in spite of the suppression it undergoes here by forming its in-medium version and dealing with its energy dependence. The GW amplitude model even admits a $1s_\eta$ bound state in ^4He with as low a binding energy as 1.2 MeV and a width of 2.3 MeV, both calculated using a static ^4He density.

Inspection of the r.h.s. of Fig. 3 reveals a trend for the three curves of calculated widths which is opposite to that observed on the l.h.s. for the calculated binding energies. Here, the GW model produces relatively small widths of order 4 MeV uniformly across the periodic table, whereas M1 and M2 give larger widths, particularly M1 with widths of order 20 MeV. This reflects partly the energy dependence of $\text{Im } f_{\eta N}(\sqrt{s})$ in the subthreshold region, which is quite distinct in each one of the three amplitude models, and partly the difference in the in-medium renormalization arising from the $\text{Re } f_{\eta N}(\sqrt{s})$ input. The latter point is readily understood by noting in Fig. 2 that the largest values of subthreshold downward energy shift are due to the GW subthreshold amplitude. This causes a particularly large reduction in the strength of the $\text{Im } f_{\eta N}(\sqrt{s})$ input for the GW amplitude model.

Table 2: Static calculations of $1s_\eta$ binding energy (B) and width (Γ) in ^{25}Mg , using three ηN amplitude models (M1, M2, GW) with (YES) and without (NO) medium corrections from Eq. (3), for several procedures of treating the energy dependence of $f_{\eta N}$. Energies and widths are given in MeV.

Eq. (3)	subthreshold	M1		M2		GW	
		B_η	Γ_η	B_η	Γ_η	B_η	Γ_η
NO	$\delta\sqrt{s} = 0$	3.2	37.4	17.3	37.8	81.8	62.7
NO	$\delta\sqrt{s} = -30$	–	–	3.0	11.2	31.2	10.0
NO	$\delta\sqrt{s}$ Eq. (5)	–	–	3.2	10.6	23.8	7.4
YES	$\delta\sqrt{s} = 0$	4.3	23.8	11.6	18.9	33.3	14.0
YES	$\delta\sqrt{s} = -B_\eta$	3.8	21.7	8.3	13.2	19.4	5.8
YES	$\delta\sqrt{s}$ Eq. (5)	–	–	2.5	7.4	14.8	3.9

Focusing on a given core nucleus, we show in Table 2 results of static-density calculations in models M1, M2 and GW of the $1s_\eta$ state in ^{25}Mg with (YES) and without (NO) employing the in-medium modification of Eq. (3). The first row in each of the YES and NO groups lists results of using threshold amplitudes: $F_{\eta N}(\sqrt{s_{\text{th}}}, \rho)$ for YES and $\tilde{f}_{\eta N}(\sqrt{s_{\text{th}}})$ for NO. The self-consistency requirement imposed by Eq. (5) is used and comparison is made within each group with another procedure applied in previous studies to incorporate energy dependence. These are (i) a fixed 30 MeV downward shift applied to the free-space ηN amplitude $f_{\eta N}(\sqrt{s})$ by Haider and Liu

(HL) [4]; and (ii) shifting down self-consistently the energy argument of the in-medium ηN amplitude $F_{\eta N}(\sqrt{s}, \rho)$ by the resultant B_η , as implemented for example by García-Recio et al. (GR) [16].

The HL procedure is compared with ours in the second and third rows of the first (NO) group, using free-space amplitudes. Both do not produce binding for the weakest amplitude M1 and practically agree for M2, while disagreeing significantly for the strongest GW amplitude. By comparing each of these rows with the first row where free-space *threshold* amplitudes are used, it is seen the effects of accounting for energy dependence are substantial in both. The GR procedure is compared with ours in the second and third rows of the second (YES) group, using *in-medium* amplitudes. The GR procedure is found to give higher binding energies and widths than ours for all amplitude models tested here, particularly for the weaker M amplitudes where it is the only one that produces a $1s_\eta$ bound state for M1. The overall effects in this group of accounting for energy dependence with respect to using in-medium threshold amplitudes (first row of the YES group), however, are less substantial than in the preceding group, particularly for the M amplitudes.

Of the three models used by us with in-medium amplitudes in Table 2 (last line), only GW provides B_η which is comparable with

$$B^{\text{exp}}(^{25}_\eta\text{Mg}) = 13.1 \pm 1.6 \text{ MeV}, \quad \Gamma^{\text{exp}}(^{25}_\eta\text{Mg}) = 10.2 \pm 3.0 \text{ MeV}, \quad (6)$$

deduced from the following $^{25}_\eta\text{Mg}$ interpretation of a peak reported by the COSY-GEM Collaboration [24]:

$$\begin{aligned} p + ^{27}\text{Al} &\rightarrow ^{25}_\eta\text{Mg} + ^3\text{He} \\ &\hookrightarrow (\pi^- + p) + X, \end{aligned} \quad (7)$$

with a decay induced by $\eta + n \rightarrow \pi^- + p$. Hence, if this peak assignment to a $1s_\eta$ state is correct,² then the underlying threshold value $\text{Re } a_{\eta N}$ must be rather large, close to 1 fm. Other procedures listed in Table 2 for treating the subthreshold ηN energy dependence require considerably smaller values of $\text{Re } a_{\eta N}$. Finally, the relatively small value of width Γ produced in the GW model should not be viewed as too restrictive since the total width must be larger than given in these models, owing to true ηNN absorption and two-pion production $\eta N \rightarrow \pi\pi N$ processes that are not accounted for by the models considered in the present work.

²This has been contested recently by Haider and Liu who offered a different interpretation of the reported peak [28].

4. Conclusions

In this work we have demonstrated the importance of, as well as the subtleties involved in constructing self-consistent η -nucleus optical potentials that incorporate the strong subthreshold energy dependence of the underlying ηN scattering amplitude. Of the three ηN amplitude models studied here self-consistently, even the relatively weak attraction in model M1 with a threshold value $\text{Re } a_{\eta N} \approx 0.2$ fm requires going down to about 35 MeV below threshold, as shown in Fig. 2, in order to calculate reliably the η -nuclear optical potential $V_\eta(\rho)$ at central nuclear densities. This downward energy shift exceeds by far the downward shifts $-B_\eta$, with $B_\eta \lesssim 20$ MeV encountered in the self-consistent calculations of García-Recio et al. [16]. The relatively large downward energy shifts in the present approach together with the rapid decrease of the free-space and in-medium ηN amplitudes lead to smaller than ever binding energies and widths with respect to those calculated in comparable models [4, 16, 17]. Thus, $^{12}_\eta\text{C}$ bound states are unlikely in models with threshold values $\text{Re } a_{\eta N} \lesssim 0.5$ fm, and as large a value as $\text{Re } a_{\eta N} \approx 0.9$ fm is required to reproduce the $^{25}_\eta\text{Mg}$ bound-state hint from the recent COSY-GEM experiment [24]. Complementarily, for as sufficiently large values of $\text{Re } a_{\eta N}$ as provided by the GW amplitude model, the calculated widths come out smaller than in other calculations.

A value of $\text{Re } a_{\eta N} \sim 0.9$ fm is likely to yield a near-threshold $^4_\eta\text{He}$ bound state, as found here using the GW amplitude model, but it is short of binding $^3_\eta\text{He}$. Stretching the limits of optical potential usage down to these light systems is of course questionable, and corresponding few-body calculations are highly needed to resolve such issues. Nevertheless, if one applies our subthreshold self-consistency scheme to η - ^3He low-energy scattering, then a very large imaginary part that might indicate a nearby virtual state is found for the η - ^3He cm scattering amplitude when using the GW amplitude model. This large imaginary part might be associated with the strong final-state interaction effects observed for the η - ^3He system [11]. In contrast to previous estimates that assigned a value of $\text{Re } a_{\eta N} \approx 0.5$ fm to describe such occurrence [29], in our self-consistent calculations it requires substantially larger values, more likely around 0.9 fm.

Acknowledgements

We thank Maxim Mai for providing us with numerical tables of ηN scattering amplitudes from Ref. [7]. A.G. thanks Colin Wilkin for useful and

stimulating correspondence. J.M. acknowledges financial support within the agreement on scientific collaboration between the Academy of Sciences of the Czech Republic and the Israel Academy of Sciences and Humanities. This work was supported by the GACR Grant No. 203/12/2126, as well as by the EU initiative FP7, HadronPhysics3, under the SPHERE and LEANNIS cooperation programs.

References

- [1] For a recent review at HYP2012, see A. Gal, Nucl. Phys. A (2013) <http://dx.doi.org/10.1016/j.nuclphysa.2013.01.011> (arXiv:1301.2145).
- [2] Q. Haider, L.C. Liu, Phys. Lett. B 172 (1986) 257.
- [3] L.C. Liu, Q. Haider, Phys. Rev. C 34 (1986) 1845.
- [4] Q. Haider, L.C. Liu, Phys. Rev. C 66 (2002) 045208.
- [5] N. Kaiser, P.B. Siegel, W. Weise, Phys. Lett. B 362 (1995) 23; N. Kaiser, T. Waas, W. Weise, Nucl. Phys. A 612 (1997) 297; T. Waas, W. Weise, Nucl. Phys. A 625 (1997) 287.
- [6] T. Inoue, E. Oset, M.J. Vicente Vacas, Phys. Rev. C 65 (2002) 035204.
- [7] M. Mai, P.C. Bruns, U.-G. Meißner, Phys. Rev. D 86 (2012) 094033.
- [8] A.M. Green, S. Wycech, Phys. Rev. C 71 (2005) 014001, and references listed therein to earlier work by these authors.
- [9] R.A. Arndt, et al., Phys. Rev. C 72 (2005) 045202; see Table I for ηN scattering-length overview.
- [10] V. Shklyar, H. Lenske, U. Mosel, Phys. Rev. C 87 (2013) 015201.
- [11] For $\eta^3\text{He}$: J. Berger, et al. (LNS-SPES4), Phys. Rev. Lett. 61 (1988) 919; B. Mayer, et al. (LNS-SPES2), Phys. Rev. C 53 (1996) 2068; T. Mersmann, et al. (COSY-ANKE), Phys. Rev. Lett. 98 (2007) 242301; J. Smyrski, et al. (COSY-11), Phys. Lett. B 649 (2007) 258; C. Wilkin, et al., Phys. Lett. B 654 (2007) 92.

- [12] For $\eta^4\text{He}$: R. Frascaria, et al. (LNS-SPES4), Phys. Rev. C 50 (1994) R537; N. Willis, et al. (LNS-SPES3), Phys. Lett. B 406 (1997) 14; A. Wrońska, et al. (COSY-ANKE), Eur. Phys. J. A 26 (2005) 421; A. Budzanowski, et al. (COSY-GEM Collab.), Nucl. Phys. A 821 (2009) 193.
- [13] S.D. Bass, A.W. Thomas, Phys. Lett. B 634 (2006) 368.
- [14] F. Pheron, et al. (MAMI), Phys. Lett. B 709 (2012) 21.
- [15] P. Adlarson, et al. (WASA@COSY Collab.), Phys. Rev. C 87 (2013) 035204.
- [16] C. García-Recio, T. Inoue, J. Nieves, E. Oset, Phys. Lett. B 550 (2002) 47.
- [17] D. Jido, H. Nagahiro, S. Hirenzaki, Phys. Rev. C 66 (2002) 045202; H. Nagahiro, D. Jido, S. Hirenzaki, Phys. Rev. C 68 (2003) 035205; D. Jido, E.E. Kolomeitsev, H. Nagahiro, S. Hirenzaki, Nucl. Phys. A 811 (2008) 158.
- [18] A. Cieplý, E. Friedman, A. Gal, D. Gazda, J. Mareš, Phys. Lett. B 702 (2011) 402.
- [19] A. Cieplý, E. Friedman, A. Gal, D. Gazda, J. Mareš, Phys. Rev. C 84 (2011) 045206.
- [20] E. Friedman, A. Gal, Nucl. Phys. A 881 (2012) 150.
- [21] D. Gazda, J. Mareš, Nucl. Phys. A 881 (2012) 159.
- [22] N. Barnea, A. Gal, E.Z. Liverts, Phys. Lett. B 712 (2012) 132.
- [23] E. Friedman, A. Gal, Nucl. Phys. A 899 (2013) 60.
- [24] A. Budzanowski, et al. (COSY-GEM Collab.), Phys. Rev. C 79 (2009) 012201(R).
- [25] T. Waas, M. Rho, W. Weise, Nucl. Phys. A 617 (1997) 449.
- [26] A. Cieplý, E. Friedman, A. Gal, J. Mareš, in preparation.
- [27] J. Mareš, E. Friedman, A. Gal, Nucl. Phys. A 770 (2006) 84.

- [28] Q. Haider, L.C. Liu, J. Phys. G: Nucl. Part. Phys. 37 (2010) 125104.
- [29] N. Willis, et al. (LNS-SPES3), Phys. Lett. B 406 (1997) 14.